Quantum Chemistry Based Force Field for Simulations of Poly(propylene oxide) and Its Oligomers

Grant D. Smith,* Oleg Borodin, and Dmitry Bedrov

Department of Materials Science and Engineering and Department of Chemical and Fuels Engineering, University of Utah, Salt Lake City, Utah 84112

Received: March 24, 1998

We present an atomistic force field for simulations of poly(propylene oxide) (PPO) and its low molecular weight oligomers. The force field is parametrized to accurately reproduce the relative conformer energies and rotational energy barriers in 1,2-dimethoxypropane (DMP) and 3,6-dimethyl diglyme (DMD) as determined from high-level ab initio electronic structure calculations. Partial atomic charges have been determined to accurately reproduce the electrostatic potential and dipole moments of important conformers of DMP and DMD as determined from quantum chemistry while yielding a charge neutral repeat unit for use in PPO simulations. The ability of the force field to accurately reproduce conformational energies is examined by comparing gas-phase molecular dynamics simulations of DMP with gas-phase NMR vicinal coupling measurements. The populations for the O−C*−C−O bond from simulations are found to be in good agreement with values determined from the experiments. The accuracy of the nonbonded interactions is examined through comparison of *PVT* data for liquid DMP from molecular dynamics simulations with experiment and predictions of DMP−water interactions using a quantum chemistry based force field for ether−water interactions with high-level ab initio calculations. In both cases good agreement is found.

Introduction

Poly(propylene oxide) (PPO) is of interest for a wide variety of applications. For example, its amorphous structure and ability to dissolve lithium salts have made PPO a leading candidate polymer electrolyte for secondary battery applications. In addition, except for short oligomers, PPO is insoluble in water, and its copolymers with water-soluble poly(ethylene oxide) (PEO) are amphiphilic. PPO/PEO copolymers are used extensively as surfactants and in biomedical applications.[1]

In previous work, we presented an atomistic force field for simulations of PEO based on quantum chemistry calculations of the conformational energetics of 1,2-dimethoxyethane (DME).[2,3] This force field has been used in simulations of DME[4] and poly(ethylene oxide)[5,6] and has been extended to include a quantum chemistry based description of ether−Li^+ interactions[7,8] and ether−water interactions.[9] In this work, we present a force field for simulations of PPO and its oligomers based upon quantum chemistry studies of conformational energetics and rotational energy barriers in 1,2-dimethoxypropane (DMP) and 3,6-dimethyl diglyme (DMD). These low molecular weight PPO oligomers are illustrated in Figure 1. The validity of the force field is demonstrated by comparison of the populations of the O−C*−C−O dihedral (C* indicating the chiral carbon center) in DMP determined from molecular dynamics simulations using the quantum chemistry based force field with estimates from gas-phase NMR vicinal coupling measurements. Intermolecular interactions are investigated by comparison of the thermodynamic properties of DMP liquid from molecular dynamics simulations with the limited amount of experimental data available. In addition, we investigate the ability of our ether−water force field, parametrized to reproduce high-level quantum chemistry energies for interaction of DME−water and demonstrated to accurately reproduce thermodynamic,[9] structural,[10] and dynamic properties[11,12] of DME/water and PEO/water solutions, to reproduce the interaction of DMP with water.

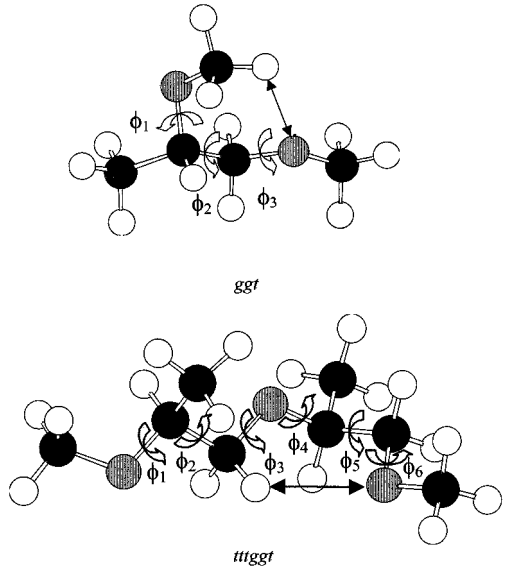

Figure 1. Lowest energy conformers of 1,2-dimethoxypropane (DMP) and 3,6-dimethyl diglyme (DMD). The backbone dihedrals, as referred to in Tables 1−4, are indicated. The arrows indicate attractive electrostatic interactions.

Quantum Chemistry Calculations

The details of our ab initio calculations of the geometries and relative conformer energies for the important conformers of DMP are provided elsewhere.[13,14] We have also examined the saddle points between important DMP conformers at the MP2/D95+(2df,p)//SCF/D95** level, consistent with our studies

10.1021/jp981599g CCC: $15.00
Published on Web 11/17/1998

TABLE 1: DMP Conformer Energies and Rotational Energy Barriers

conformer	SCF geometry[a] kcal/mol	MP2 geometry[a] kcal/mol	force field kcal/mol
ggt	0.00	0.00	0.00
ttt	−0.04 (0.16)	−0.06 (0.14)	0.21
gtt	0.20 (0.40)	0.21 (0.41)	0.47
tgt	0.72	0.77	0.83
tḡg	0.92	0.81	0.99
gḡt	0.97		1.14
tḡt	1.06	1.03	0.89
tgḡ	1.11		1.15
gḡg	1.17		1.09
ttḡ	1.28 (1.48)		1.37
ggg	1.41		1.22
ḡtt	2.38 (2.58)		2.57
ttt−gtt	0.86 (1.06)		0.98
tgt−ggt	0.92		1.06
ggt−gtt	2.02 (2.12)		2.19
ttt−ttḡ	2.04 (2.24)		2.28
ttt−tgt	3.13 (3.23)		3.01
ttt−tḡt	4.26 (4.36)		4.21
ḡtt−ttt	4.52 (4.72)		5.03
gtt−ḡtt	6.28 (6.48)		6.55
tgt−tḡt	9.30		9.11
ttg−ttḡ	9.82 (10.02)		10.02

[a] MP2/D95+(2df,p) energies, relative to ggt, at MP2/D95** or SCF/D95** geometries. Energies in parentheses are adjusted according to the text.

TABLE 2: DMP Conformer and Barrier Geometries

	ab initio[a]			force field		
conformer	ϕ_1	ϕ_2	ϕ_3	ϕ_1	ϕ_2	ϕ_3
ggt	**−76.5**	**76.5**	**−178.9**	−79.1	83.4	−178.5
ttt	**−165.3**	**176.1**	**−179.9**	−161.1	174.5	179.3
gtt	**−86.5**	**173.1**	**178.2**	−87.9	177.2	178.2
tgt	**−149.7**	**74.3**	**−173.2**	−155.0	74.3	−177.6
tḡg	**−166.7**	**−79.1**	**75.8**	−164.3	−80.0	82.6
gḡt	−75.4	−65.9	179.3	−81.9	−66.7	−179.9
tḡt	**−168.8**	**−74.8**	**176.4**	−164.7	−71.4	178.4
tgḡ	−153.0	68.5	−98.2	−156.7	83.2	−84.0
gḡg	−84.0	−72.7	82.0	−83.0	−77.1	82.2
ttḡ	−164.4	176.5	−85.8	−161.9	179.2	−83.1
ggg	−80.4	72.5	86.1	−78.0	82.6	85.4
ḡtt	74.7	167.8	−178.8	68.6	168.0	−179.3
ttt−gtt	−118.4	175.8	179.0	−120	175.8	178.9
tgt−ggt	−131.6	70.9	−173.6	−127	74.6	−177.7
ggt−gtt	−78.2	123.5	178.3	−82.0	129	179.9
ttt−ttḡ	−164.3	175.2	−117.9	−161.7	174.8	−122
ttt−tgt	−157.8	118.1	−178.5	−157.8	121	−178.5
ttt−tḡt	−161.9	−122.2	177.8	−159.0	−125	178.8
ḡtt−ttt	122.8	170.8	−178.0	122	172.2	179.9
gtt−ḡtt	3.0	171.8	−179.8	2	175.8	179.3
tgt−tḡt	−150.8	−2.9	−179.4	−155.9	−1	180.0
ttg−ttḡ	−161.3	160.5	6.0	−161.8	151.1	9

[a] Bold indicates MP2/D95** geometries; otherwise SCF/D95** values are given. Dihedrals are defined in Figure 1 and are in units of degrees.

of the conformer energies in DMP[13,14] and the conformer and barrier energies in DME.[2] In the latter study, basis set size and electron correlation effects on conformer energies and geometries were systematically investigated. The relative conformer energies and rotational energy barriers at this level of theory, and selected conformer energies determined with MP2/D95** geometries, are summarized in Table 1. The respective conformational geometries are given in Table 2. These calculations were performed using Gaussian 94.[15]

The relative conformer energies in DMP have been considered in detail elsewhere.[13,14,16] For the purposes of developing an atomistic force field, it is of value to compare the salient conformational characteristics of DMP with those of DME. The pendent methyl group in DMP has important consequences on both conformer energies and rotational energy barriers. Unlike DME, the g^+ and g^- conformations of the C−O−C*−C bond, of the O−C*−C−O bond, and of the C*−C−O−C dihedrals are not equivalent in DMP because of the chiral carbon center. In labeling conformers, we use the standard g and notation (for example, see ref 13). Although the energetics for rotation about the C*−C−O−C dihedral are quite similar to those for the C−C−O−C bond in DME, the characteristics of the C−O−C*−C bond differ considerably from those for the C−C−O−C DME dihedral. These differences are due to steric interactions between the methoxy group and the pendant methyl group in DMP. In DME, the gtt conformer is almost 1.5 kcal/mol higher in energy than the ttt. In contrast, the energy of the DMP gtt conformer is only slightly greater than that of the ttt conformer (see Table 1) because the methoxy−methyl steric interactions in the latter conformer. The energy of the O−C*−C−O gauche conformations (tgt and tt) are higher in DMP than in DME (tgt) by more than 0.5 kcal/mol relative to the respective ttt conformers because of attractive methyl−oxygen electrostatic interactions in the DMP ttt conformer. The DMP ggt conformer energy is comparable to the that of the ttt conformer because of strong attractive 1,5 C(H)···O electrostatic interactions, as were found in DME for the tg^+g^- conformers and also in other alkyl ethers.[17,18]

Another important influence of methoxy−methyl steric effects on the energetics of the C−O−C*−C dihedral is that the ttt−gtt and tgt−ggt barriers in DMP are less than 1 kcal/mol, much lower than any barrier between important conformers in DME. This is not due to an intrinsic lowering of the rotational barrier resulting from the presence of the methyl group (e.g., relative to the gtt conformer the ttt−gtt barrier is comparable in DME and DMP) but rather to an increase in the relative energy of the DMP ttt conformer due to the methoxy−methyl steric interactions. These low barriers may have important ramifications for the dynamics of PPO and its oligomers. Other rotational energy barriers in DMP between important conformers are comparable to those in DME (>2 kcal/mol).

TABLE 3: DMD Conformer Energies and Rotational Energy Barriers

conformer	SCF geometry[a] kcal/mol	force field kcal/mol
tttggt	0.00	0.00
ggtttt	0.05	−0.01
tttttt	0.12 (0.32)	0.32
ttttgt	0.55	0.61
tgtttt	0.80	0.97
tḡgttt	0.53	0.38
tggttt	1.57	1.67
ttgḡtt	0.67 (0.87)	0.89
ttḡggt	0.83	0.85
tttgtt	0.20 (0.40)	0.25
tttḡtt	[2.58]	2.34
tggttt−tgtttt	2.41	2.23
ttḡggt−tttggt	1.08	1.26
ttḡgtt−tttgtt	1.10 (1.30)	1.32
tggttt−tgḡttt	5.43	5.33
tttggt−ttttgt	0.71	0.90
tttgtt−tttḡtt	5.89 (6.09)	6.17
tttgtt−tttttt	0.89 (1.09)	0.93
tttḡtt−tttttt	[4.72]	5.15

[a] MP2/D95+(2df,p) energies, relative to tttggt, at SCF/D95** geometries. Energies in parentheses were adjusted according to the text. Energies in brackets are from analogous conformations of DMP and were used in parametrization of the DMD torsions.

TABLE 4: DMD Conformer and Barrier Geometries

	ab initio[a]						force field					
conformer	ϕ_1	ϕ_2	ϕ_3	ϕ_4	ϕ_5	ϕ_6	ϕ_1	ϕ_2	ϕ_3	ϕ_4	ϕ_5	ϕ_6
ttttt	−159.0	175.0	172.9	−160.9	−175.0	180.0	−160.9	175.2	173.5	−161.2	174.6	179.6
ttttgt	−161.8	173.8	177.5	−146.0	70.5	−175.2	−161.9	174.4	170.1	−158.4	72.6	−177.7
tttggt	−159.7	173.7	179.7	−97.1	68.5	−176.7	−160.9	174.5	−172.5	−75.7	84.0	−177.3
tgtttt	−144.7	72.1	−171.0	−152.2	176.1	179.4	−155.1	74.1	−170.3	−155.6	174.5	179.0
tg$\bar{g}$ttt	−163.6	−68.4	100.2	−149.2	178.5	−179.3	−163.9	−72.6	96.1	−150.8	177.9	−179.6
ggtttt	−92.6	70.5	−178.1	−153.4	176.0	179.7	−78.6	83.4	−174.9	−155.3	175.0	179.4
tggttt	−151.3	67.9	88.6	−149.8	176.4	178.9	−156.0	70.3	84.5	−150.4	174.5	179.3
tt$\bar{g}$gtt	−164.6	174.6	−93.1	−90.6	174.0	179.0	−161.6	177.1	−87.2	−89.5	176.2	178.7
tt$\bar{g}$ggt	−163.9	175.3	−94.8	−95.1	68.6	−175.1	−160.5	176.3	−110.4	−84.6	79.8	−177.3
tttgtt	−158.4	175.3	178.4	−91.6	173.8	179.0	−160.5	175.2	172.5	−87.9	177.5	178.7
tggttt−tgtttt	−147.7	67.7	115.5	−158.5	175.7	179.3	−155.7	72.9	115	−161.3	174.6	179.2
tt$\bar{g}$gtt−tttggt	−163.3	176.1	−110.5	−89.9	68.2	−175.5	−160.8	176.3	−110	−84.6	79.8	−177.3
tt$\bar{g}$gtt−tttgtt	−163.5	175.9	−115.6	−82.6	174.4	179.1	−161.3	175.4	−116	−79.8	176.5	178.6
tttggt−ttttgt	−161.1	174.1	179.6	−129.3	69.5	−174.9	−162.0	173.9	175.7	−129	73.1	−177.5
tggttt−tg$\bar{g}$ttt	−160.7	74.6	−7.8	−134.3	178.0	−179.9	−160.9	79.9	−8	−144.7	177.8	−179.9
tttgtt−ttt$\bar{g}$tt	−159.3	174.4	174.5	3.1	171.5	−179.7	−161.1	174.7	175.0	3	174.8	179.4
tttgtt−ttttt	−158.6	175.6	−179.2	−119.3	176.2	179.4	−160.9	175.3	177.8	−119	176.3	179.4

[a] SCF/D95** geometries. Dihedrals are defined in Figure 1 and are in units of degrees.

Examination of higher molecular weight PPO oligomers, such as DMD (see Figure 1), reveals that C*−C−O−C* and [C*]−C−O−C*−C dihedrals, which are not present in DMP, are manifest in the longer chains. Although the former is unique to DMD and higher molecular weight oligomers, the latter can be expected to be similar to the C−O−C*−C dihedral in DMP. To parametrize the torsional potential for these dihedrals, we have examined selected conformers and rotational energy barriers for DMD. The MP2/D95+(2df,p) energies for these conformers are given in Table 3, while the SCF/D95** geometries are given in Table 4. Comparison with Tables 1 and 2 indicate that the energies and geometries of the DMP conformers are consistent with those for analogous conformers of DMP (e.g., compare DMP ggt and DMD tttggt).

TABLE 5: Nonbonded Force Field Parameters for DMP and DMD

pair (ij)	A_{ij} kcal/mol or kcal Å^{12}/mol	B_{ij} Å^{-1}	C_{ij} kcal Å^6/mol
	$E_{ij} = A_{ij}\exp(-B_{ij}r_{ij}) - C_{ij}r_{ij}^{-6}$		
C−C	14976	3.090	640.8
O−O	75845	4.063	398.9
H−H	2650	3.740	27.4
C−H	4320	3.415	138.2
O−C	33702.	3.577	505.6
O−H	14176	3.902	104.5
	$E_{ij} = A_{ij}r_{ij}^{-12} - C_{ij}r_{ij}^{-6}$		
C−O_W	1419603		1168.6
O−O_W	658665		958.9
H−O_W	198857		247.8

Force Field Parametrization

As discussed in our previous work[14] Boltzmann weighting of the various DMP conformers using the quantum chemistry based energies in Table 1 yields a trans fraction (f_t) for the O−C*−C−O bond somewhat greater than that determined from gas-phase NMR vicinal coupling measurements. It was shown that when the energy of the DMP conformers with O−C*−C−O dihedrals in the trans state was increased by 0.2 kcal/mol, the resulting Boltzmann populations of the O−C*−C−O were in good agreement with experimental results.[14] This energy difference is within our estimated uncertainty in the relative ab initio conformer energies of ±0.3 kcal/mol from basis set limitations, approximate methods for electron correlation effects, zero-point vibrational effects, and thermal vibrational and rotational effects. We therefore have parametrized the force field with respect to the adjusted conformational energies given in parentheses in Table 1.

Nonbonded Parameters. We have employed the same repulsion/dispersion parameters in our description of DME[3] and PEO in our force field for DMP and DMD, summarized in Table 5. The partial atomic charges for DMP were determined as follows. The electrostatic potential for a grid of approximately 12 000 to 15 000 points each for the SCF/D95** geometries of the DMP tgt and tg and DMD tgtttt, tttggt, and ggtttt conformers, plus the MP2/D95** geometries of the DMP ttt and ggt conformers, were determined using MP2/D95+(2df,p) wave functions. The grid extended from 1.8 Å from each hydrogen and oxygen atom and 2.5 Å from each carbon atom to a distance of 3.5 Å from any atom. Inclusion of more distant points and denser grids was found to have little influence on the calculated partial charges. A least-squares procedure was employed to determine the partial atomic charges that gave the best representation of the potential at the grid points for each conformer, subject to the constraints of a charge neutral repeat unit and "equivalent" atoms having equal charge, as indicted in Figure 2. The charges obtained for each conformer where then averaged to yield the partial charges indicated in Figure 2. These charges yield dipole moments for each conformer which are consistently larger than, but within 10% of, the MP2/D95+-(2df,p) dipole moments.

Valence Parameters. The bond stretching and valence angle bending force constants were taken from previous work,[2,1] as were the equilibrium bond lengths. The equilibrium valence angles for bends involving hydrogen atoms were also taken from previous work. The remaining parameters were determined to yield the best agreement of the valence geometries with the DMP ttt and ggt conformer geometries determined at the MP2/D95** level. The valence parameters are summarized in Table 6. A comparison of geometries is shown in Table 7.

Torsional Parameters. Quantitative modeling of conformational properties of DMP and DMD, and subsequently of PPO, necessitates an accurate representation of the conformational energies (static and dynamic properties) and rotational energy barriers (dynamic properties). As mentioned above, the conformational energetics of DMP differ significantly from those of DME. It is likely that the very different properties of these

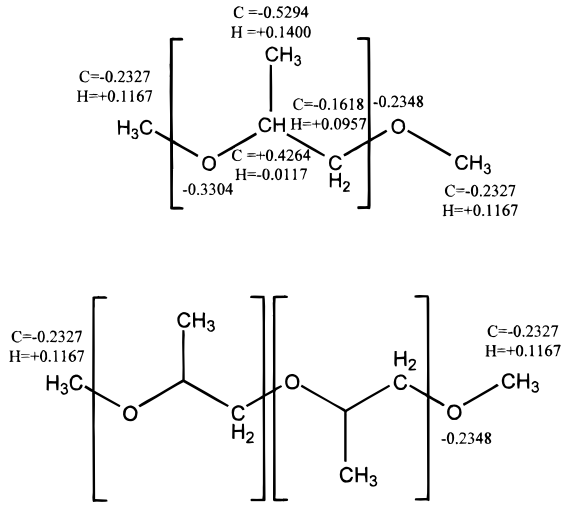

Figure 2. Partial atomic charge assignment for DMP and DMD. The charge neutral PPO repeat unit is indicated. "Equivalent" atoms are constrained to have equal charges.

TABLE 6: Valence Force Field Parameters

$E_{ij} = 0.5k_{ij}(r_{ij} - r_{ij}^0)^2$

stretch	k_{ij} kcal Å^{-2}/mol	r_{ij}° Å
C−O	739	1.4
C−H	655	1.09
C−C	618	1.52

$E_{ijk} = 0.5k_{ijk}(\Theta_{ijk} - \Theta_{ijk}^\circ)^2$

bend	k_{ijk} kcal rad^{-2}/mol	Θ_{ijk}° rad
C−O−C*	149	1.9065
C−O−C	149	1.8908
O−C−H	112	1.9211
O−C*−C(H_2)	119	1.8791
O−C*−C(H_3)	119	1.9402
O−C−C*	119	1.8493
C−C−H	85.8	1.9109
C−C−C	108	1.9431
H−C−H	77	1.8902

molecules and their corresponding polymers (e.g., solubility in aqueous solution) is, to a large extent, a consequence of these differences. We have therefore attempted to reproduce the conformer energies and rotational energy barrier in DMP and DMD as obtained from high-level quantum chemistry calculations with the same degree of accuracy as was done for DME.

The torsional parameters for DMP and DMD are given in Table 8. The parameters in bold face, with the exception of the O−C−C−H parameter, were adjusted to match the quantum chemistry values for conformer and energy barriers in DMP given in Table 1. The parameters in italics were adjusted to match the quantum chemistry energies for DMD given in Table 3. As expected, the parameters for the [C*]−C−O−C*−C dihedral are quite similar to those for the DMP C−O−C*−C dihedral. The O−C−C−H 3-fold potential was adjusted to yield a rotational energy barrier of 2.83 kcal/mol for rotation

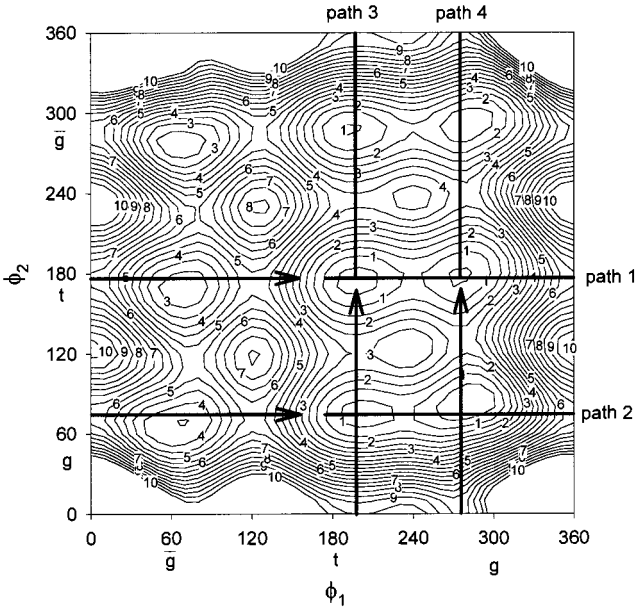

Figure 3. Conformational energy of $\phi_1\phi_2$t conformers of DMP from molecular mechanics calculations using the quantum chemistry based force field. Low-energy paths for rotational isomerization are illustrated schematically. Energies are in kcal/mol relative to the ggt conformer.

of the pendent methyl group as obtained from MP2/D95+-(2df,p)//SCF/D95** calculations for ttt DMP. The remaining parameters were taken from previous work.[2,19] The molecular mechanics force-field energies for the conformers and rotational energy barriers can be compared to the quantum chemistry values in Tables 1 and 2 for DMP and DMD, respectively, while the geometries can be compared in Tables 2 and 4. The agreement between molecular mechanics and quantum chemistry values is good. The ability of the DMP based potential function to accurately predict conformational energies in DMD (with parametrization of the additional functions to describe interactions not present in DMP) indicates that the force field should do a good job of describing higher molecular weight oligomers and PPO.

We have generated a conformational contour map of the conformational energy surface for $\phi_1\phi_2$t conformers of DMP, shown in Figure 3. The low-energy paths between important conformers are illustrated schematically. Path 1 involves $\phi_1$tt conformations, while path 2 involves $\phi_1$gt conformations. These paths, as well as the quantum chemistry conformer and rotational barrier energies, are shown in Figure 4. The molecular mechanics force field accurately reproduces the quantum chemistry path. Similar agreement is seen for path 3 (tϕ_2t) and path 4 (gϕ_2t) in Figure 5.

Gas-Phase Populations

Gas-phase populations of the O−C*−C−O dihedral in DMP have been estimated from proton NMR vicinal coupling measurements.[20] At 403 K, these were determined to be $f_t = 0.39 \pm 0.01$, $f_g = 0.41 \pm 0.01$, and $f_{\bar{g}} = 0.20 \pm 0.01$. We

TABLE 7: DMP Valence Geometries[a]

conformer	C−O	O−C*	C*−C-(H_2)	C−O	O−C	C*−C-(H_3)	C−O−C*	O−C*−C-(H_2)	C*−C−O	C−O−C	O−C*−C-(H_2)	C−C*−C
ttt (qc)	1.421	1.430	1.523	1.422	1.420	1.526	113.0	104.5	108.1	111.2	112.8	111.8
ttt	1.409	1.413	1.537	1.413	1.407	1.530	113.6	106.3	108.8	111.2	111.3	111.5
ggt (qc)	1.427	1.427	1.525	1.424	1.420	1.524	114.2	112.6	109.8	111.1	106.1	110.4
ggt	1.409	1.409	1.541	1.413	1.407	1.525	114.0	111.1	109.3	111.2	107.6	110.5

[a] From MP2/D95** optimized geometry. Bond lengths in angstroms and valence angles in degrees.

TABLE 8: Torsional Parameters for DMP and DMD

torsion	k_1 kcal/mol	k_2 kcal/mol	k_3 kcal/mol
$E = 0.5[k_1(1 - \cos \phi_{ijkl}) + k_2(1 - \cos 2\phi_{ijkl}) + k_3(1 - \cos 3\phi_{ijkl})$			
C−O−C*−C(H_2)	**−0.50**[a]	**−0.24**	**−1.13**
C−O−C*−C(H_3)	**−0.14**	**0.12**	
O−C−C−O	**−0.29**	**−2.44**	**−0.74**
C−C*−C−O	**1.97**	**0.03**	
C*−C−O−C	**0.485**	**−0.34**	**−0.34**
O−C−C−H			**−0.34**
C*−C−O−C*	*3.09*[b]	*1.02*	*0.50*
[C*]−C−O−C*−C	*−0.58*	*−0.07*	*−1.13*
C−C−C−H			−0.28
H−C−C−H			−0.28
C−O−C−H			−0.81

[a] Parametrized against DMP conformational energies. [b] Parametrized against DMD conformational energies.

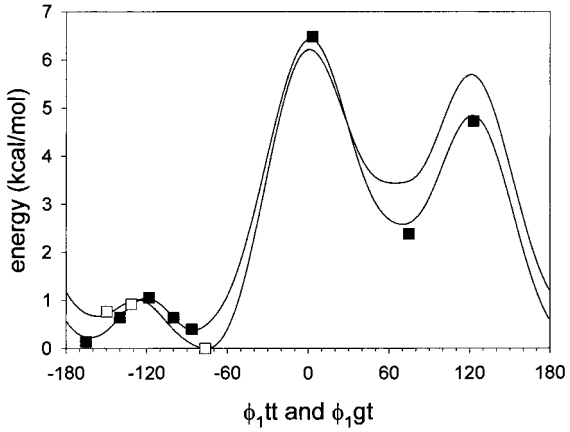

Figure 4. Low-energy paths for rotational isomerization in DMP. The solid curves are from molecular mechanics calculations using the quantum chemistry based force field. The filled squares are quantum chemistry energies for the $\phi_1$tt path (path 1, Figure 3), while the empty squares are values for the $\phi_1$gt (path 2, Figure 3) path.

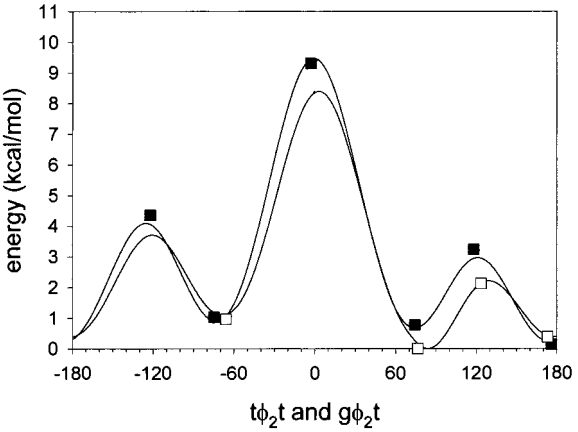

Figure 5. Low-energy paths for rotational isomerization in DMP. The solid curves are from molecular mechanics calculations using the quantum chemistry based force field. The filled squares are quantum chemistry energies for the tϕ_2t path (path 3, Figure 3), while the empty squares are values for the gϕ_2t (path 4, Figure 3) path.

performed molecular dynamics simulations of an ensemble of 192 DMP molecules in the gas phase at 400 K, employing our quantum chemistry based force field and a stochastic dynamics algorithm described elsewhere.[21] Conformational sampling was performed for 600 ps after 300 ps of equilibration. The resulting populations for conformers whose population is greater than 1% are given in Table 9. Also shown are the populations resulting from Boltzmann weighting of the conformers using the force field energies in Table 1. The gas-phase MD populations yield $f_t = 0.41$, $f_g = 0.41$, and $f_{\bar{g}} = 0.18$, in good agreement with the experimental values. For most conformers the gas-phase simulation and Boltzmann populations are in good agreement. The $\phi_1\bar{g}g$ conformers experience significant conformational constrains due to interactions of the end methyl group with the pendent methyl, accounting for the significantly reduced populations. The gtt and tgt conformers, on the other hand, are in quite shallow minima, as illustrated in Figures 3 and 5. As a result, the population of these conformers is greater than expected from Boltzmann weighting.

TABLE 9: Gas-Phase DMP Populations (400 K)

conformer	MD	Boltzmann	MD/Boltzmann
ggt	0.203	0.217	0.94
ttt	0.191	0.167	1.14
gtt	0.145	0.120	1.21
tgt	0.102	0.076	1.34
t$\bar{g}$t	0.056	0.070	0.80
g$\bar{g}$t	0.045	0.051	0.88
tg$\bar{g}$	0.046	0.051	0.90
tt$\bar{g}$	0.042	0.037	1.13
t$\bar{g}$g	0.028	0.063	0.44
ggg	0.033	0.046	0.72
gt$\bar{g}$	0.030	0.031	0.97
g$\bar{g}$g	0.022	0.054	0.41
tgg	0.015	0.014	1.07

DMP Liquid Simulations

In future papers we will report on the thermodynamics, conformations, and structure of DMP and PPO in the neat liquid. For purposes of testing the validity of the nonbonded (intermolecular) interactions, comprised of the dispersion/repulsion + Coulomb interactions, we have performed molecular dynamics simulations of neat DMP liquid and compared *PVT* properties with experiment. The paucity of experimental data precludes an extensive comparison. The only experimental data we could discover in the literature was a density of 0.855 g/cm^3 at 293 K.[22] We performed simulations on a system of 192 molecules at 293 K using the algorithm described elsewhere.[21] After 1.2 ns of equilibration, a 0.2 ns *NPT* simulation yields a mean density of 0.832 g/cm^3, in good agreement with experimental results.

DMP−Water Interactions

In previous work we parametrized an ether−water force field for simulations of ethers and poly(ethers) in aqueous solution.[9] The interaction of water and DME was determined from quantum chemistry for a number of geometries, and the Lennard-Jones interaction parameters between C, H, and O of the ether with the TIP4P water center (O_W) were determined. The resulting force field (which also includes electrostatic interactions between water and ether based on partial atomic charges) was found to accurately reproduce thermodynamic,[9] structural,[10,12] and dynamic[11,12] properties of DME/water and PEO/water solutions. We investigated the ability of this ether−water force field to represent the interaction of DMP−water by determining the binding energy of tgt DMP and water as a function of separation between the water oxygen atom and the center of the C*−C bond in DMP. This binding consists of dispersion/repulsion effects that are represented by our previously derived ether−water force field and electrostatic interactions (hydrogen bonding and polar interactions) that are dependent upon the partial atomic charges for DMP. The latter were determined from quantum chemistry as described above.

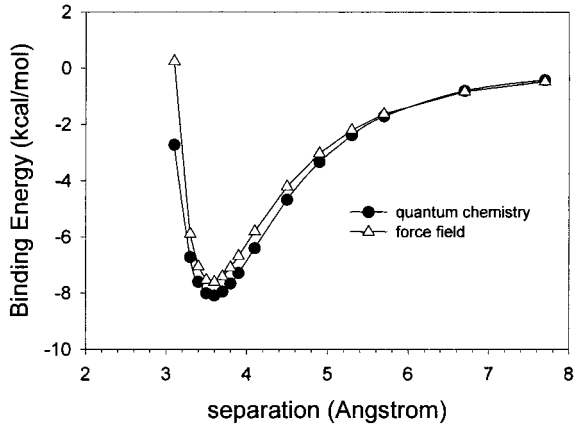

Figure 6. Binding in of water to tgt DMP as a function of separation. Quantum chemistry values are MP2/D95+(2df,p) energies. The geometries were determined by changing the separation from the optimal complex geometry while maintaining fixed ether and water internal geometries.

The quantum chemistry and force field interaction energies for DMP−water are compared in Figure 6. The good agreement seen between the force field predictions and quantum chemistry for DMP−water indicates that the ether/water force field previously developed has more general applicability than just DME−water and PEO−water systems, provided that the electrostatic potential (partial atomic charges) of the ether of interest is accurately parametrized.

Acknowledgment. The authors gratefully acknowledge support from the National Science Foundation—Division of Materials Research through Grant DMR 9624475.

References and Notes

(1) Harris, J. M. *Poly(Ethylene Glycol) Chemistry: Biotechnical and Biomedical Applications*; Plenum Press: New York, 1992.
(2) Jaffe, R. L.; Smith, G. D.; Yoon, D. Y. *J. Phys. Chem.* **1993**, *97*, 12745.
(3) Smith, G. D.; Jaffe, R. L.; Yoon, D. Y. *J. Phys. Chem.* **1993**, *97*, 12752.
(4) Smith, G. D.; Jaffe, R. L.; Yoon, D. Y. *J. Am. Chem. Soc.* **1995**, *117*, 530
(5) Smith, G. D.; Yoon, D. Y.; Jaffe, R. L.; Colby, R. H.; Krishnamoorti, R.; Fetters, L. J. *Macromolecules* **1996**, *29*, 3462.
(6) Smith, G. D.; Yoon, D. Y.; Wade, C. G.; O¢Leary, D.; Chen, A.; Jaffe, R. L. *J. Chem. Phys.* **1997**, *106*, 3798.
(7) Smith, G. D.; Jaffe, R. L.; Partridge, H. *J. Phys. Chem. A* **1997**, *101*, 1705.
(8) Smith, G. D.; Borodin, O.; Pekny, M.; Annis, B.; Londono, D.; Jaffe, R. L. *Spectrachim. Acta* A **1997**, *53*, 1273.
(9) Bedrov, D.; Pekny, M.; Smith, G. D. *J. Phys. Chem. B* **1998**, *102*, 996.
(10) Bedrov, D.; Borodin, O.; Smith, G. D., *J. Phys. Chem.*, submitted.
(11) Bedrov, D.; Smith, G. D. In preparation.
(12) Borodin, O.; Bedrov, D.; Trouw, F.; Smith, G. D. In preparation.
(13) Smith, G. D.; Crain, K.; Jaffe, R. L. *J. Phys. Chem. A* **1997**, *101*, 3152.
(14) Smith, G. D.; Jaffe, R. L.; Yoon, D. Y. *Chem. Phys. Lett.*, submitted
(15) Frisch, M. J.; Trucks, G. W.; Schlegel, H. B.; Gill, P. M. W.; Johnson, B. G.; Robb, M. A.; Cheeseman, J. R.; Keith, T.; Petersson, G. A.; Montgomery, J. A.; Raghavachari, K.; Al-Laham, M. A.; Zakrzewski, V. G.; Ortiz, J. V.; Foresman, J. B.; Cioslowski, J.; Stefanov, B. B.; Nanayakkara, A.; Challacombe, M.; Peng, C. Y.; Ayala, P. Y.; Chen, W.; Wong, M. W.; Andres, J. L.; Replogle, E. S.; Gomperts, R.; Martin, R. L.; Fox, D. J.; Binkley, J. S.; Defrees, D. J.; Baker, J.; Stewart, J. P.; Head-Gordon, M.; Gonzalez, C.; Pople, J. A. *Gaussian 94*, revision D.1; Gaussian, Inc.: Pittsburgh, PA, 1995.
(16) Sasanuma, Y. *Macromolecules* **1995**, *28*, 8629.
(17) Law, R. V.; Sasanuma, Y. *J. Chem. Soc., Faraday Trans.* **1996**, *92*, 4885.
(18) Law, R. V.; Sasanuma, Y. *Macromolecules* **1998**, *31*, 2335.
(19) Smith, G. D.; Yoon, D. Y. *J. Chem. Phys.* **1994**, *100*, 649.
(20) Sasanuma, Y. *J. Phys. Chem.* **1994**, *98*, 13486.
(21) Smith, G. D.; Yoon, D. Y.; Jaffe, R. L. *Macromolecules* **1993**, *26*, 298.
(22) Sigma-Aldrich Regulatory & Safety Data, www.sial.com, 1(1), 213B.